



# Synthesis and Characterization of Co-doped Nickel-ZnO/Polypyrrole Nano-composites, and Their Effect on Photo-catalytic Degradation of P-nitrophenol under Solar Irradiation

Gemechu Lemessa<sup>1\*</sup>, Dunkana Negussa<sup>1</sup> and P. S. Bedi<sup>1</sup>

<sup>1</sup>Department of Chemistry, Wollega University, P.O.Box: 395, Nekemte, Ethiopia.

## Authors' contributions

This work was carried out in collaboration between all authors. All authors read and approved the final manuscript.

## Article Information

DOI: 10.9734/IRJPAC/2018/45731

### Editor(s):

- (1) Dr. Wolfgang Linert, Professor, Institute of Applied Synthetic Chemistry, Vienna University of Technology Getreidemarkt, Austria.
- (2) Dr. Chenyi Wang, Associate Professor, School of Materials Science and Engineering, Changzhou University, Wujin District, Changzhou, Jiangsu Province, China.
- (3) Dr. Farzaneh Mohamadpour, Department of Organic Chemistry, University of Sistan and Baluchestan, Iran.

### Reviewers:

- (1) Tsamo Cornelius, University of Maroua, Cameroon.
- (2) Oh Seok Kwon, Korea Research Institute, Korea.
- (3) Kate Kotlhao, Vaal University of Technology, South Africa.

Complete Peer review History: <http://www.sciencedomain.org/review-history/28004>

Original Research Article

Received 02 October 2018  
Accepted 20 December 2018  
Published 29 December 2018

## ABSTRACT

Nickel-polypyrrole co-modified ZnO nano-composites (Ni-ZnO/Ppy) were synthesized by two methods, metal impregnation of nickel (Ni) and In-situ chemical polymerization of polypyrrole (Ppy) on ZnO nano-particles. The crystal size, band gap energy and bond structure of as-synthesized nano-composites were investigated by using x-ray diffraction(XRD),UV-Vis and Fourier transform infrared (FT-IR) spectroscopic techniques respectively. Photo-catalytic degradation efficiency of synthesized photo-catalysts was investigated on p-nitrophenol dyes under solar irradiations and Co-doped photo-catalysts shows better catalytic degradation efficiency than both ZnO and Ni-ZnO nano-particles. Ni-ZnO/Ppy photo-catalysts effectively degraded 96.04% of p-nitrophenol dye on 180 minute visible light irradiation. Highest photo-catalytic activity of Ni-ZnO/Ppy nano-composites over ZnO photo-catalysts was attributed due dopants to the lower rate of recombination of the photo generated electrons- holes as well as its lower crystal size and band gap energy. The photo-catalytic degradation of p-nitrophenol kinetically follows pseudo first-order reactions for Ni-ZnO/Ppy photo-catalysts.

\*Corresponding author: E-mail: [gemechulemecha@gmail.com](mailto:gemechulemecha@gmail.com);

**Keywords:** Co-doped photo-catalyst; Kinetic degradation, nano-composite; p-nitrophenol.

## 1. INTRODUCTION

One of the major challenges of a developing country like Ethiopia is solving environmental issue with newly booming industries in different industrial zones and costs of waste water treatment especially from wastes from textile and leather industries. The textile industry is amongst all the industries in Ethiopia is the largest consumer of high quality fresh water and with the nature of their production processes significantly contributing to pollution. Wastewater from the textile industry is also a significant environmental pollution source of persistent organic pollutants. Not only textile wastewater but also textile products often contain chemicals such as formaldehyde, azo-dyes, dioxins, pesticides and heavy metals, which might pose a risk to humans and the environment. These compounds have been found in wastewater after home washing, in organic solvent after dry-cleaning and also in the atmosphere after incineration [1].

In recent years, photo-catalytic degradation of organic pollutants in water and air using semiconductor materials has received more attention. Under light irradiation, the semiconductor generates electron/hole pairs, with electrons excited from the valence band to the conduction band and leaving positive holes in the valence band. Therefore, photo generated holes in the valence band and photo generated electrons in the conduction band are formed, respectively. The generated electron/hole pairs initiate a complex series of oxidative and reductive reactions on the surface of the semiconductor. Organic pollutants adsorbed on the surface of the semiconductor are partly or completely degraded [2].

Among the semiconductors,  $\text{TiO}_2$  is the most widely used for photo-catalysis due to its high photo-catalytic activity, non-toxicity, and good stability. ZnO as a potential semiconductor with similar band gap energy to  $\text{TiO}_2$  and ZnO exhibit a better efficiency than  $\text{TiO}_2$  in photo-catalytic degradation of some contaminations are receiving more attention [3]. To overcome these disadvantages, significant efforts has been devoted to preventing the recombination of photo-generated hole/electron pairs and improving the utilization efficiency of solar light during photo-catalytic reactions by doping with metals and surface modification by polymers gets attention to solve the challenge of catalytic

efficiency and stability of photo-catalysts [4]. Polypyrrole (Ppy), as a traditional conducting polymer, is widely used in batteries, super capacitors, electrochemical or biological sensors, conductive textiles and fabrics, actuating mechanism, electromagnetic screen, anti-static paint and drug delivery systems. Besides superior conductivity, electrochemical reversibility and high polarizability, Ppy displays good chemical and thermal stability to avoid being dissolved in acidic and neutral solution, and under goes only slight photo-catalytic degradation in ambient atmosphere due to oxidation [3-5]. Thus the present study has been designed to increase efficiency of photon harvesting by reducing band gap energy of bare ZnO nano-particles by co-modification with metal, nickel(Ni) and conduction polymers, polypyrrole and its photo-catalytic activities of p-nitrophenol was investigated under visible irradiation.

## 2. MATERIALS AND METHODS

### 2.1 Synthesis of Ni-ZnO Materials

The Ni-doped ZnO is prepared by a modified homogeneous precipitation using zinc acetate, oxalic acid and nickel chloride as precursors [5]. Then 4.8 g of zinc acetate and 2.5 g of oxalic acid were dissolved in 50 ml of distilled water under stirring for 2h at room temperature. An amount of nickel chloride, which corresponds to Ni to ZnO molar ratio equal to 1, 5 and 10%, respectively was added to the solution. The obtained precipitate was filtered, washed with methanol, dried in an oven at 80°C for 24 h, and then heated at 400°C for 3 h to get a Ni doped zinc oxide (Ni-ZnO) [5,11].

### 2.2 Synthesis of Ni-ZnO/Ppy Nano-composites

The Ni-ZnO/Ppy composites were prepared by the direct impregnation method [16]. In a typical procedure, 1 g of Ni-ZnO nano-particles was dispersed in 10% M.wt of 30 mL of aqueous Ppy solution during one hour-stirring. The obtained Ni-ZnO/Ppy nano-composite powders were filtered, washed three times with ethanol and water respectively, and dried for 24 h at 80°C. Then dried precipitate was calcinated in furnace at 500°C for 2 hours.

### 2.3 X- Ray Diffraction (XRD) Analysis

The average crystallite size of the as-synthesized Ni-ZnO and Ni-ZnO/Ppy nano-composites was calculated using the Debye-Scherrer formula [8-12].

$$D = \frac{0.9 \lambda}{\beta \cos \theta}$$

where D is the average crystallite size,  $\lambda$  is the wavelength of the X-ray = 0.15406 nm for Cu target K $\alpha$  radiation,  $\beta$  is the full width at half – maximum of an XRD peak and  $\theta$  is the Bragg's angle.

### 2.4 UV–Vis Absorption Spectral Analysis

Band gap energy (eV) of as–synthesised photo-catalysts was obtained using the equation given below [9,10].

$$E_g \text{ (eV)} = \frac{1240}{\lambda} \text{ eV}$$

Where,  $E_g$  is band gap energy in electron volts and  $\lambda$  is wavelength (nm) corresponding to absorption edge

### 2.5 Photo-catalytic Degradation Studies

250 ml of dye solution was mixed with a given amount of photo-catalyst and allowed to equilibrate for 30 min in the dark to obtain adsorption/desorption equilibrium before irradiating the dye in the reactor. The solution was separately done under visible irradiation sources and magnetically stirred. Air was continuously bubbled through the reactor tube.

5 mL of each reaction mixture was withdrawn at 20 minutes time interval. The suspension was centrifuged at 3000 rpm for 5 minutes and filtered off to remove the catalyst particles and absorbance of p-nitrophenol solution was determined spectrophotometrically at 325 nm. Percentage degradation of nitrophenol was calculated using the relation [6].

$$\% \text{ Degradation} = \frac{A_0 - A_t}{A_0} \times 100$$

Where,  $A_0$  is absorbance of dye at initial stage,  $A_t$  is absorbance of dye at time "t".

### 2.6 Photo-catalytic Reactor

The photo-catalytic reactor consists of a quartz tube with an inlet tube for provision of air purging

during photo-catalysis and outlet tube for the collection of samples from the reactor at regular time intervals.

The Visible lamp (Philips) with definite power of 40W, 220 V, 0.18 A and 50 Hz frequency was employed as visible source, and positioned 9 cm above and parallel to the reactor [8,12].

### 2.7 Factors Affecting Efficiency Photo-catalyst

#### 2.7.1 Effect of Ph

Effect of pH for degradation of p-nitrophenol on synthesized photo-catalytic was investigated over a pH range from 3 to 12 keeping other parameters constant.

#### 2.7.2 Effect of catalyst load

The effect of catalyst load on photo-catalytic degradation of p-nitrophenol was observed by taking different amounts of Ni-ZnO/Ppy / (35 mg to 175 mgL<sup>-1</sup>) each time at constant dye concentration (16 mgL<sup>-1</sup>) and pH of 3.

#### 2.7.3 Effect of dye initial concentration

The effect of initial concentrations of p-nitrophenol for degradation on synthesized photo-catalyst was observed by taking different dye initial concentrations 16 mgL<sup>-1</sup> to 80 mgL<sup>-1</sup>, and by fixing other parameters constant (photo-catalyst load =175 mgL<sup>-1</sup>, pH = 3).

#### 2.7.4 Effect of irradiation time

The relation between the percent degradation of p-nitrophenol with irradiation time was studied over a reaction time of 180 minutes, using optimized concentration of dye 16 mgL<sup>-1</sup>, photo-catalyst load 175 mgL<sup>-1</sup> and pH of 3.

### 2.8 Kinetic Degradation Studies

The kinetics of the photo-catalytic degradations of p-nitrophenol solutions was investigated using optimized photo-catalysts load (175 mgL<sup>-1</sup>), dye initial concentration (16 mgL<sup>-1</sup>) and pH=3 under visible light irradiations. The graph was plotted for each case with  $\ln C_0/C_t$  as a function of time (t). Where,  $C_0$  is the initial concentration of dye and  $C_t$  is concentration of dye at time t. From the slope of the respective plots, the rate of photo-catalytic degradation of p-nitrophenol was determined.

### 3. RESULTS AND DISCUSSION

#### 3.1 X- Ray Diffraction (XRD) Analysis

The XRD patterns of calcinated ZnO and Ni-ZnO and Ni-ZnO/Ppy nano-particles were shown in Fig. 1(A, B and C) respectively. The diffraction peaks at scattering angle in Figure.1C ( $2\theta$ ); 32.125°, 34.481°, 36.525°, 47.483°, 57.117°, 63.058° and the corresponding Miller indices are (100), (002), (101), (102), (110) (103) and (112) respectively for Ni-ZnO/Ppy nano-particles.

Whereas in Fig. 1b ( $2\theta$ ); 31.837°, 34.479°, 36.495°, 47.480°, 56.724° and 62.891° corresponding to the reflection from crystal planes for as –synthesized Ni-ZnO respectively and also both the synthesized photo-catalysts are suggesting hexagonal crystal structure [7-12].

The most intense peak at  $2\theta$ ; 27.480° for Ni-ZnO/Ppy in Fig. 1(C), 36.525° for Ni-ZnO in Fig. 1 (B) and 36.429° for ZnO nano-particles, Fig. 1 (A) as shown in their XRD patterns were used to calculate the average crystalline size. The values of calculated average crystallite size (D) of the photo-catalysts are given in Table 1. As Debye-Scherrer formula calculation shows, the higher crystalline size obtained was 37.35 nm for ZnO

then 31.47 nm for Ni-ZnO nano-particles. However, the lowest crystalline size was obtained for co-doped Ni-ZnO/Ppy nano-composite which is 18.23 nm. Doping with metals like nickel and conducting polymer, polypyrrole may reduce the size and help to control the morphology of synthesized nano-composites similar reported [9].

**Table 1. Average crystalline size (D) of as-synthesized Ni-ZnO and Ni-ZnO/Ppy nano-composites photo-catalysts**

Sample	$2\theta$ (degree)	$\beta$ (radian)	D(nm)
ZnO	36.429	0.00408	37.35
Ni-ZnO	36.525	0.00490	31.47
Ni-ZnO/Ppy	27.4801	0.0051	18.23

#### 3.2 Fourier Transform Infrared (FT-IR) Spectroscopic Study

Fig. 2A shows the FT-IR spectrum of the ZnO, and Ni-ZnO and Ni-ZnO/Ppy over 400-4000  $\text{cm}^{-1}$ . IR spectroscopy gives qualitative information about the way in which the adsorbed Polypyrrole (Ppy) molecules and Nickel metals are bonded to the surface of ZnO nano-particles. Fig. 2B and Fig. 2C compares the IR spectra of Ni-ZnO and Ni-ZnO/Ppy nano-composites.

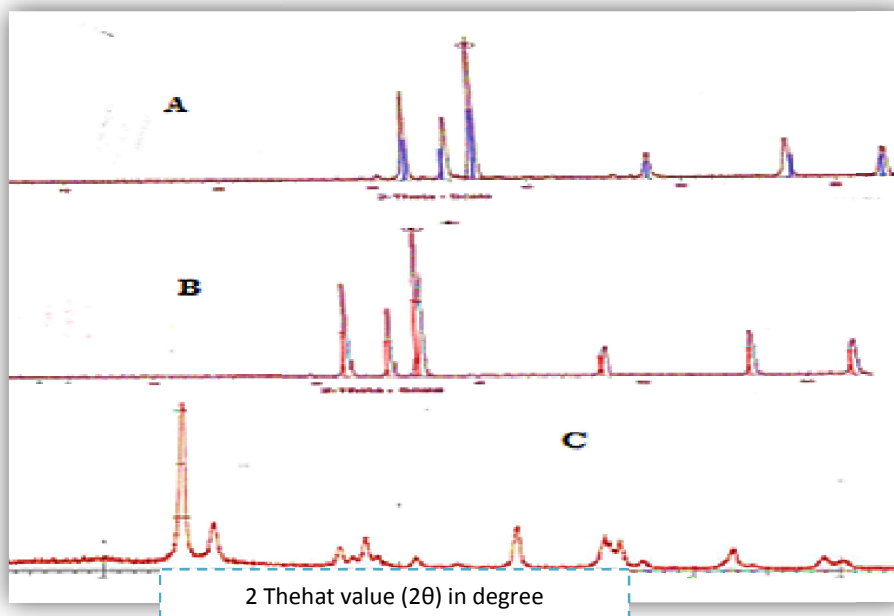


**Fig. 1. XRD spectral of; A) ZnOnano-particles, B) Ni-ZnOnano-particles and C) Ni-ZnO/Ppy nano-composite**

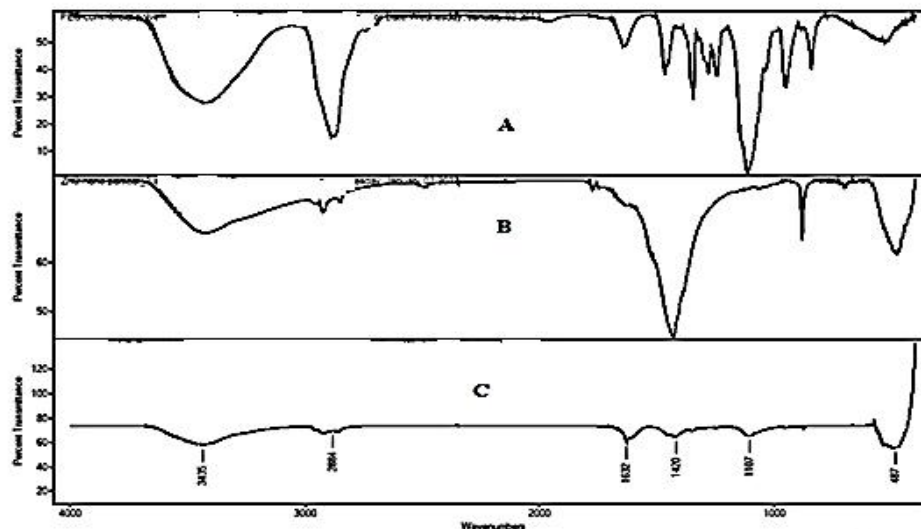


**Fig. 2. FTIR spectra of (A) ZnO, (B) Ni-ZnO nano-particles and (C) Ni-ZnO/Ppy nano-composite respectively**

From Fig. 2 comparing, Fig. 2(C) with Fig. 2(B), it could be found that for the Ni-ZnO nano-composite there is a new absorption peak at  $1107\text{ cm}^{-1}$ , which can be attributed to the flex vibrations of  $\text{CH}_2\text{-O-Zn}$  [4, 9]. It demonstrated that ZnO nano-particles bonded with Ppy.

The absorption peak at  $2853\text{ cm}^{-1}$  in ZnO Fig. 2(A). That corresponds to  $2856\text{ cm}^{-1}$  in Ni-ZnO/Ppy Fig. 2(C) is due to the CH group stretching vibration shifts to higher wave length the case of Ni-ZnO nano-particles. The broad band peak appearing at  $3435\text{ cm}^{-1}$  for Ni-ZnO/Ppy in Fig. 2(C) due to OH group, has shifted higher wave numbers in comparison with the hydroxyl group peak in the ZnO nano-particles ( $3429\text{ cm}^{-1}$ ). It indicates that covalent bonds have been formed between the Ppy,  $\text{Ni}^{+2}$  and ZnO nano-particles in Ni-ZnO/Ppy [17].

The strong absorption band formed at the  $483\text{ cm}^{-1}$  for ZnO in Fig. 2(a) correlated to metal oxygen bond in ZnO is shifted to lower wave length for ZnO,  $480\text{ cm}^{-1}$  for Ni-ZnO in Fig. 2(C). The peaks in the range of  $1400\text{-}1500\text{ cm}^{-1}$

corresponds to the C=O bonds. The most intense absorption peak at  $1431\text{ cm}^{-1}$  in Fig. 3a and  $1420\text{ cm}^{-1}$  in Fig. 2(C) due to O-C-O stretching of mono-dentates carbonates originated during synthesis of ZnO nano-particle. The adsorbed band at  $1635\text{ cm}^{-1}$  is assigned O-H bending vibrations. The intense peak at  $1800\text{-}1600\text{ cm}^{-1}$  corresponds to C=O stretching frequency and  $700\text{-}990\text{ cm}^{-1}$  is due to C-H bending vibrations respectively.

### 3.3 UV-Vis Absorption Spectral Analysis

The optical absorption of ZnO nano-particles, Ni-ZnO and Ni-ZnO/Ppy nano-composite are given in Fig. 3. The adsorption edge for ZnO, Ni-ZnO and Ni-ZnO/Ppy nano-particles are obtained at  $383\text{ nm}$ ,  $418\text{ nm}$  and  $510\text{ nm}$  respectively. The band gaps of the synthesised photo-catalyst, Ni-ZnO and Ni-ZnO/Ppy nano-composites are well extended to visible region of spectrum as compared to ZnO nano-particles (Table 2). This may be due to the modification of electronic levels of ZnO by  $\text{Ni}^{+2}$  and Ppy as similarly reported [8,9,14].

**Table 2. Absorption on wavelength and band gaps energy of ZnO and Ni-ZnO and Ni-ZnO/Ppy nano-composite photo-catalysts**

Photo-catalysts nano-particles	Wavelength in (nm)	Band gap energy ( $E_g$ ) in (ev)
ZnO (calcinated)	383	3.23
Ni-ZnO	418	2.96
Ni-ZnO/Ppy	510	2.43

Band gap energy of (eV) of Ni-ZnO/Ppy is less than that of Ni-ZnO and ZnO nano-particles. Thus, absorption peaks of ZnO were shifted from 383 nm to 418 nm and 510 nm wavelength for Ni-ZnO and Ni-ZnO/Ppy respectively. As compared to bare ZnO nano particle both nano composites were shifted to visible region. The extension of absorption in the visible range can be attributed due to the nickel doping. Additional co-doping Ni-ZnO by polypyrrole (Ppy) account further shift in wave length of nano composites to visible region as seen Fig. 3 of Table 2. The narrowing band gap energy of former nano composites Ni-ZnO/Ppy are due to delocalized Ni 3d states of doped Ni, intermix with O 2p of ZnO and Ppy of Nitrogen (N) 2p states of photo-catalyst ZnO. Such intermixing of doped metal 3d and ppy, N 2p states with energy states of photo-catalyst near valence band (VB) narrows down

the band gap energy of photocatalyst [18]. Further reduction in the band gap of the Ni-ZnO/Ppy nano composites might be due to the synergetic effect of the two dopants; Ppy and Ni<sup>+2</sup> generating electrons to reduce the band gaps [7,9,16,17].

### 3.4 Atomic Adsorption Spectroscopic (AAS) Analysis

Table-3 shows the observed data for AAS analysis for Ni-ZnO and Ni-ZnO/Ppy nano-composites photo-catalysts. Fairly good correlation ( $R^2 = 0.998$ ) to the AAS data of the synthesized photo catalysts was found from AAS calibrations curve linear equations,  $y = 0.013 x + 0.032$ ; as shown in Fig. 4. Where y is absorbance and x is the concentration of Nickel in ppm per samples.

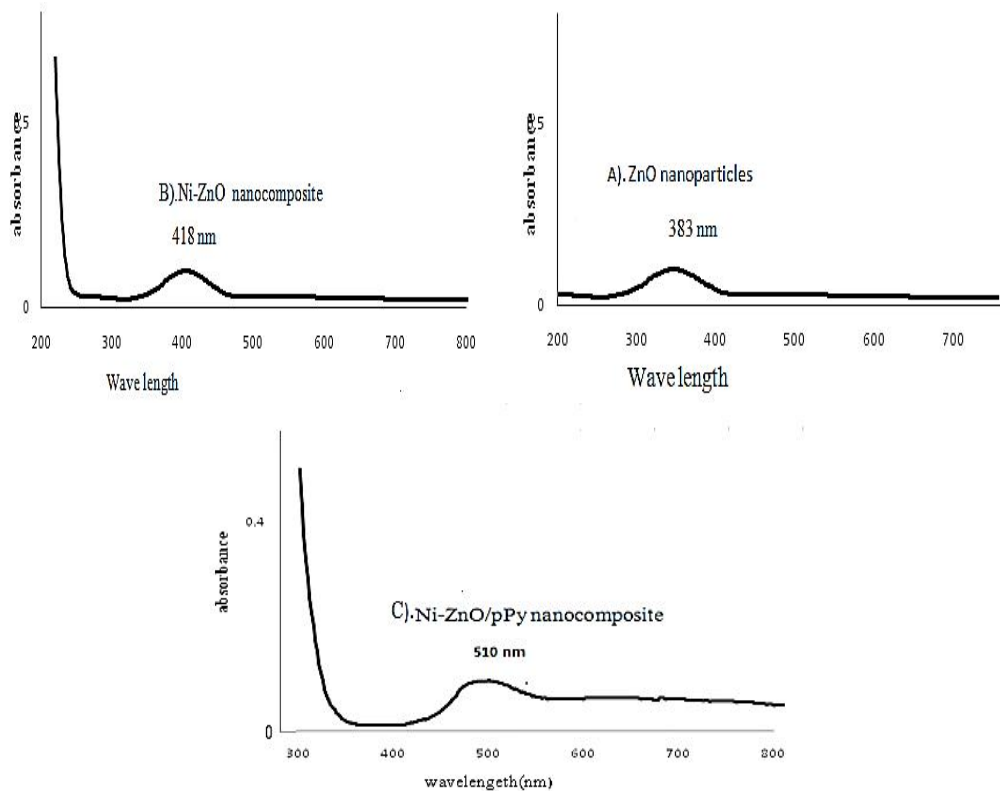


Fig. 3. UV-Visible diffuse absorption spectra and the absorption edge wavelength a) ZnO nano-particles, b) Ni-ZnO, c) Ni-ZnO/Ppy nano-composites

Table 3. Zinc concentration in the as-synthesized Ni-ZnO and Ni-ZnO/Ppy nano-composite

Photo-catalysts at (20 mg)	Element	Absorbance	Concentration (ppm)	% metal
Ni-ZnO	Ni	0.809	59.77	59.77
Ni-ZnO/Ppy	Ni	0.735	54.07	54.07

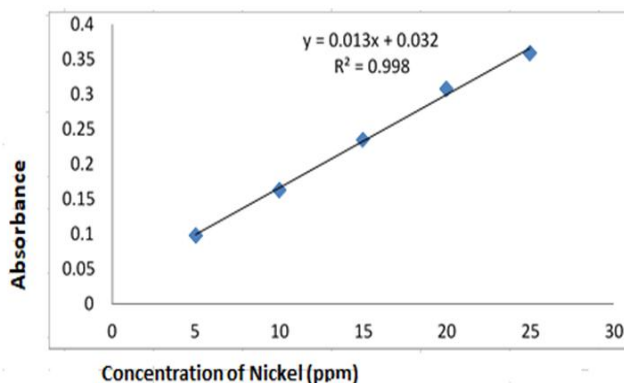


Fig. 4. AAS Calibration curve for Nickel

### 3.5 Factors Affecting Efficiency of Photo-catalysts

#### 3.5.1 Effect of photo-catalyst load

Series of experiments were carried out to find the optimum amount by varying its amount the photo-catalysts (Ni-ZnO/Ppy) load from  $1$  to  $175\text{mgL}^{-1}$ . To achieve highest photo-catalytic reaction rate, the optimum amount of the photo-catalysts was set to  $175\text{mgL}^{-1}$  as shown in Fig. 5. The observed dependence of reaction rate on the amount of photo-catalysts can be explained in terms of the availability of active sites at the adsorbent surface and the level of light penetration possibly through the reaction medium. With increasing the amount of photo-

catalysts up to  $175\text{mgL}^{-1}$  the percent degradation dyes were increased with in increasing the adsorbent total surface area and thus, the number of active sites made available for the photo-catalytic reaction to take place very easily. However, increasing excess photo-catalysts (above the optimal load) may account for inducing more aggregation (particle-particle interactions) between photo-catalysts and also accounts for reducing photon penetration through the sample and reduces removal abilities of photo-catalysts. The degradation efficiency decreases after achieving an optimum value of photo-catalyst load [8,9]. Therefore,  $175\text{mgL}^{-1}$  of photo-catalyst was selected as the optimum amount of the Ni-ZnO/Ppy nano-composites photo-catalyst for the subsequent experiments.

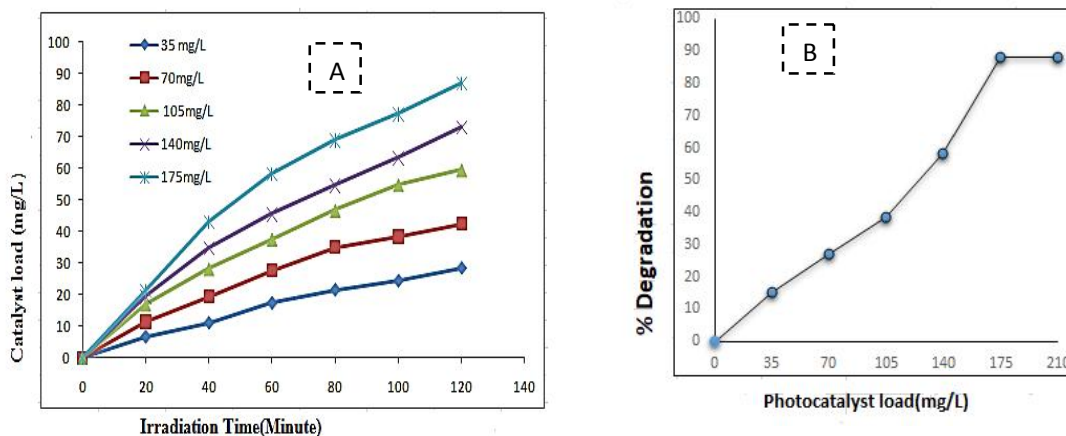


Fig. 5(A). Plot of catalyst load versus visible light irradiation times for degradation of p-nitrophenol at optimized parameters like (Dye =  $16\text{mgL}^{-1}$ , pH = 3), Fig. 5 (B). Plot of percent degradation of p-nitrophenol versus Ni-ZnO/Ppy photo-catalyst load



### 3.5.2 Effect of pH

The pH of solutions greatly affects the rate of reaction taking place on a semiconductor surfaces due to its influences on the surface-charge-properties of the photo-catalysts. The effect of on pH on the photo-catalytic degradation rate of para-nitrophenol was investigated in the range of pH 3.0 –12.0. The photo-degradation efficiency of synthesized photo-catalysts was investigated on p-nitrophenol dye probe solution with an initial concentration of  $16 \text{ mgL}^{-1}$  using Ni-ZnO/Ppy nano-composites photo-catalyst ( $175 \text{ mgL}^{-1}$ ) show maximum degradation at acidic medium pH=3. The highest photo-catalytic degradation of p-nitrophenol was observed at pH = 3.0 as shown in Fig. 6.

### 3.5.3 Effect of initial dye concentration

The photo-degradation efficiency of synthesized photo-catalysts was investigated on p-nitrophenol dye probe solution with an initial concentration of  $16 \text{ mgL}^{-1}$  using Ni-ZnO/Ppy nano-composites photo-catalyst ( $175 \text{ mgL}^{-1}$ ) show maximum degradation at acidic medium pH = 3 as show in Fig. 7. As the dye concentration was increased degradation activity is kept constant and then little decrease in degradation activity of photo-catalysts was observed as similarly reported [8, 9]. At higher dye initial concentration, the approach of the radiation photons to the catalyst surface is hindered and screened off, thereby, reducing the photo-catalytic activity in the system [12]. Moreover, at the higher dye concentration, the number of collisions between dye molecules increases at the cost of required collisions between dye molecules and OH radical and therefore, the rate of reaction is retarded [13,22].

### 3.5.4 Photo-catalytic degradation study

Photo catalytic degradations of p-nitrophenol on synthesized photo catalysts, Ni-ZnO/Ppy was higher than Ni-ZnO and lesser in case of ZnO nano particles comparatively. This could be due to the slightly lower particle size of the former may accounts for high degradation activities than Ni-ZnO nano particle photo catalysts. In addition doping nickel and polypyrrole on surface of ZnO nano particles reduces the band gap energy modified once and also the both dopant nickel and polypyrrole under solar irradiation generates electrons to conduction band of ZnO which accounts best photocatalytic action of co-doped ZnO nano composites under solar irradiation. Thus, the n-electron of polypyrrole after receiving solar radiation due to lower band gap than ZnO particles, they generated electrons create new energy levels between conduction and valence bands of ZnO, thus, decreasing the band gap in zinc oxide[15]. The observed highest degradation of p-nitrophenol over Ni-ZnO/Ppy photo catalysts were due to dopants Ppy and Ni that can account for better performance co-doped photo catalysts.

### 3.5.5 Mechanism for degradation of dyes on synthesized photo-catalyst

Under visible light irradiation, both nickel and Ppy absorbed the visible light and induced excited-state electrons. The photo-excited electrons were injected into the conduction band of ZnO nano-particles, The electron in the conduction band ( $e^-$ CB) of ZnO nano-particle is transferred to molecular oxygen, leading to the formation of  $\cdot\text{OH}$  and  $\cdot\text{O}_2^-$  radicals, which are active oxidizers capable of degrading organic pollutants and oxidized the dye contaminations as shown in proposed mechanism in Fig. 8.

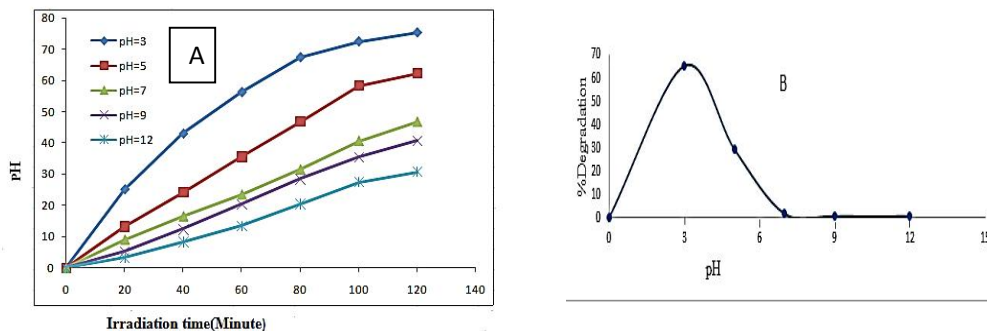


**Fig. 6 (A).** Plot of pH versus visible light irradiation time for degradation of p-nitrophenol  
**Fig. 6(B).** Plot of percent degradation of p-nitrophenol as function of pH under visible light irradiation at fixed other parameters of (Dye =  $16 \text{ mgL}^{-1}$ , Ni-ZnO/Ppy =  $175 \text{ mgL}^{-1}$ )



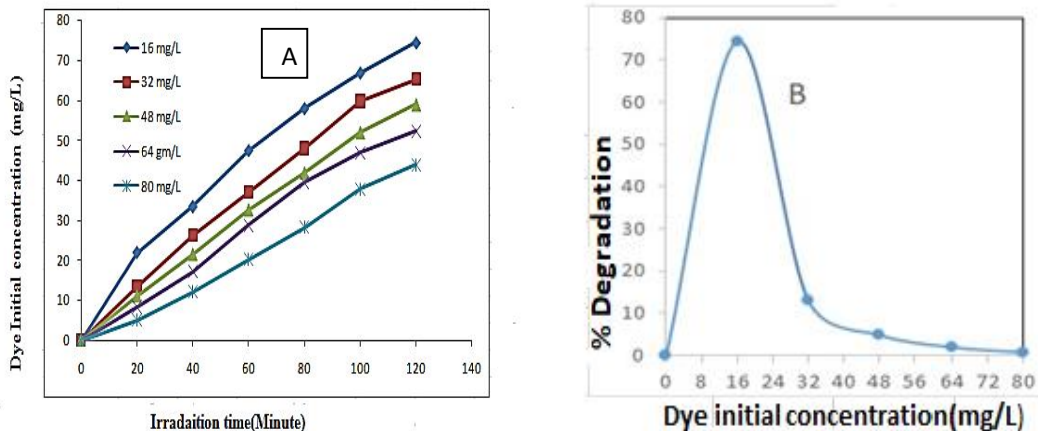


Fig. 7 (A). Plot of dye initial concentration versus visible light irradiation for degradation of para-nitrophenol

Fig. 7(B). Plots of percentage degradation of para-nitrophenol as a function of Dye initial concentration under Visible light irradiation (at constant Ni-ZnO/Ppy load of  $175 \text{ mgL}^{-1}$  and  $\text{pH} = 3$ )

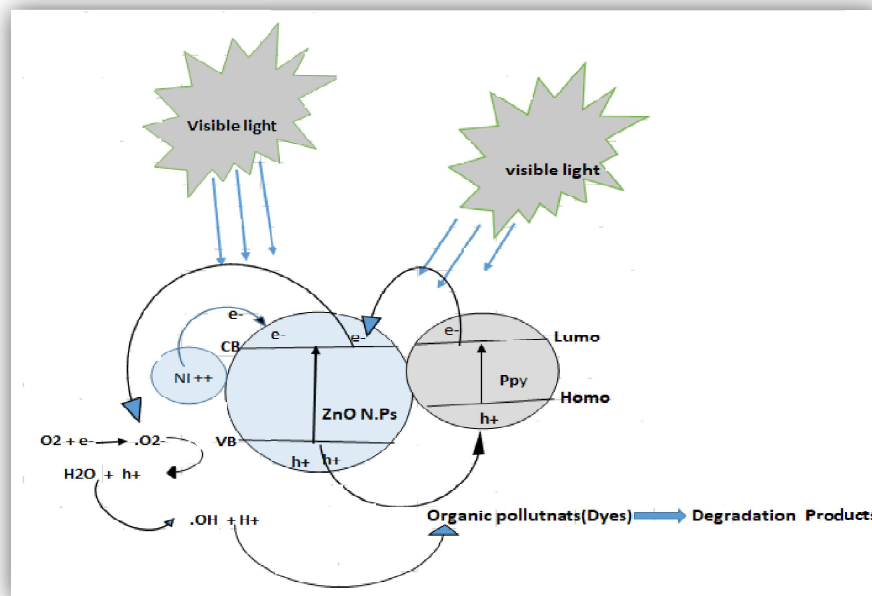


Fig. 8. Proposed mechanism of photo-catalytic activities of Ni-ZnO/Ppynano-composite under visible radiation in aqueous solution

The result shows that the percent photo-catalytic degradations of p-nitrophenol at 180 min contact time under visible radiation using ZnO, Ni-ZnO and Ni-ZnO/Ppy nano-particles are 7.35 and 83.37 and 96.04%, respectively (Fig. 9). Higher photo-catalytic degradation activities Ni-ZnO/Ppy nano-particles photo-catalysts on p-nitrophenol dye is due to co-doping of ZnO, both metal

doping by Ni and surface modification by conducting polymers, polypyrrole contributes positively, in enhancing the photo-catalytic degradation of the substrate p-nitrophenol [19-21]. Also, nickel traps the electrons at the conduction band and prevents electro-hole recombination [22].

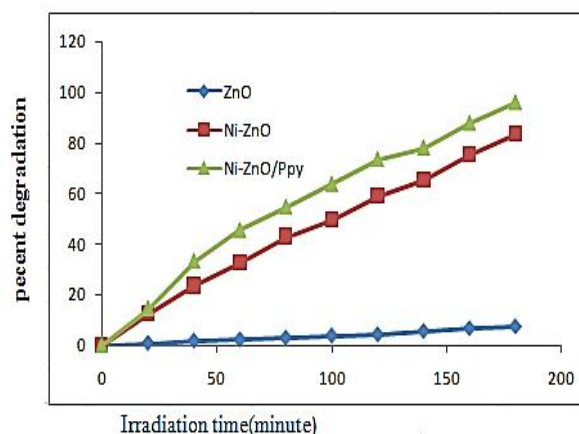


Fig. 9. Plot of percentage degradation of p-nitrophenol as a function of time under visible irradiations by photo-catalysts, ZnO, Ni-ZnO and Ni-ZnO/Ppy nano-composite

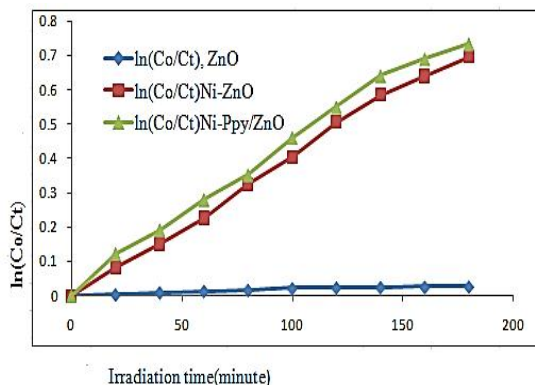


Fig. 10. Plot of  $\ln(C_0/C_t)$  versus irradiation time for photo-catalytic degradation of 4-NPs using under Visible irradiation at (dye initial concentration =  $16 \text{ mgL}^{-1}$ , photo-catalyst load =  $175 \text{ mgL}^{-1}$ , pH = 3)

### 3.6 Kinetic Studies of Photo-catalytic Degradation

The adsorption rate constants of 4-NPs degradations under visible irradiation using Ni-ZnO and Ni-ZnO/Ppy photo-catalysts were obtained as;  $4.33 \times 10^{-4}$  and  $5.39 \times 10^{-3} \text{ min}^{-1}$ , respectively as shown in Fig. 10. Fairly good correlations to the pseudo-first Order adsorption and photo-catalytic degradation reaction kinetics were obtained for all cases [18,21].

### 4. CONCLUSION

Present study concludes that doping of Ni in ZnO reduces  $e^- - h^+$  recombination and implies high energy harvesting effect for photo-catalytic degradation of p-nitrophenol. 83.31 and 96.04% of p-nitrophenol were degraded over Ni-ZnO and

Ni-ZnO/Ppy nano-composite photo-catalyst under solar radiation respectively. Enhanced photo-catalytic activities of Ni-ZnO/Ppy a nano-particle is due to dopants, Nickel and polypyrrole under solar irradiation they generate electrons to conduction bands of ZnO nano particles and enhances photo-catalytic activities of Ni-ZnO/Ppy and photo-catalytic degradation of p-nitrophenol follows pseudo-first order reaction mechanism.

### COMPETING INTERESTS

Authors declare that no competing interests exist among them.

### REFERENCES

1. Križanec B, Majcen Le Marechal, Dioxins A, Dioxin-like. Persistent organic pollutants

- in textiles and chemicals in the textile sector. *Croatia Chemical Acta*. 2006; 79(2):177-186.
2. Xu XL, Duan X, Yi ZG, Zhou ZW Fan XM, Wang Y. Photo-catalytic production of superoxide ion in the aqueous suspensions of two kinds of ZnO under simulated solar light. *Catalysis Communications*. 2010;12(1):169–172.
  3. Palominos RA, Mondaca MA, Giraldo A, Penuela G, Perez-Moya M, Mansilla HD. Photo-catalytic oxidation of the antibiotic tetracycline on TiO<sub>2</sub> and ZnO suspensions. *Catalysis Today*. 2009;144(1):100–105.
  4. Nabiyouni G, Barati A, Saadat M. Surface adsorption of polyethylene glycol and polyvinyl alcohol with variable molecular weights on zinc oxide nanoparticles. *Journal of Chemical Engineering*. 2011;8: 1-29.
  5. Xin Li, Peng Wang, Baibiao Huang, Xiaoyan Qin, Xiao Yang Zhang, Qianqian Zhang. Precisely locate Pd-Polypyrrole on TiO<sub>2</sub> for enhanced hydrogen production. *International Journal of Hydrogen Energy*. 2017;42:15-25.
  6. Habib MA, Shahadat MT, Bahadur NM, Ismail IM, Mahmood AJ. Synthesis and characterization of ZnO-TiO<sub>2</sub> nano-composites and their application as photo-catalysts. *International Nano Letters*. 2013; 3(1):1-5.
  7. Chen LC, Tu YJ, Wang YS, Kan RS, Huang CM. Characterization and photoreactivity of N-, S-, and C-doped ZnO under UV and visible light illumination. *Journal of Photochemistry and Photobiology A: Chemistry*. 2008;199:170–178.
  8. Mohamed FN, Samira S, Ali R, Noomen M, Ammar H. Enhanced photo-catalytic performance of Ni-ZnO/Polyaniline composite for the visible light driven hydrogen generation. *Journal of the Energy Institute*. 2018;14(1):204-570.
  9. Temesgen Achamo, Yadav OP. Removal of 4-nitrophenol from water using Ag–N–P-Tri-doped TiO<sub>2</sub> by photo-catalytic oxidation technique. *Department of Chemistry. Libertas Academica*. 2018; 11(1):29-34.
  10. Yirga Brhane, Abi Tadesse. Synthesis and characterization of Cr-N-P-TRI doped ZnO nano-particles for photo-catalytic degradation of malachite green under visible radiation. *Research Journal of Pharmaceutical, Biological and Chemical Sciences*. 2018;9(3):10-22.
  11. El-Kemary M, El-Shamy H, El-Mehasseb I. Photocatalytic degradation of ciprofloxacin drug in water using ZnO nano-particles. *J. Lumin*. 2010;130:27–31.
  12. Zhu C, Wang L, Kong L, Yang X, Zheng S, Chen F, Maizhi F, Zong H. Photo-catalytic degradation of azo dyes by supported TiO<sub>2</sub> + UV in aqueous solution. *Chemosphere*. 2000;41:303-309.
  13. Lodha S, Vaya D, Ameta R, Punjabi P. Photo-catalytic degradation of phenol red using complexes of some transition metals and hydrogen peroxide. *J. Serb. Chem. Soc*. 2008;73:631-639.
  14. Tesfay Welderfael, Yadav OP, Abi MT, Jyotsna Kaushal. Synthesis, characterization and photo-catalytic activities of Ag-N-co-doped ZnO nano-particles for degradation of methyl red, *Bull. Chem. Soc. Ethiop*. 2013;27(2):221-232.
  15. Ren C, Yang B, Wu VX, Fu JZI, Guo YT, Zhao Y, Zhu CJ. Synthesis of Ag/ZnO nano-rods array with enhanced photo-catalytic performance, *Hazard. Mater*. 2010;182:123.
  16. Shao TH, Chi JC, Mu HH. Improved photo-catalytic performance of ZnO nanogras decorated pore-array films by surface texture modification and Silver nanoparticle deposition. *Journal of Hazardous Material*. 2011;198:307-316.
  17. Amir Mostafaeia, Ashkan Zolriasatein, Synthesis and characterization of conducting polyaniline nano composites containing ZnO nano rods, *Materials International*. 2012;22(4):273–280.
  18. Alebel Nibret, Yadav OP, Isabel Diaz, Abi M. Tadesse. Cr-N co-doped ZnO nano particles: Synthesis, characterization and photocatalytic activity for degradation of thymol blue, *Bull. Chem. Soc. Ethiop*. 2015;29(2):247-258.
  19. Dan Zhao, Chuncheng Chen, Yifeng Wang, Wanhong MA, Jincan Zhao, Tijana Rajh, Ling Zang. Enhanced photocatalytic degradation of dye pollutants under visible irradiation on Al(III)-modified TiO<sub>2</sub>: Structure, interaction, and interfacial electron transfer, *environ. Sci. Technol*. 2008;42:308–314.
  20. Rauf MA, Meetani MA, Hisaindee S. An overview on the photocatalytic degradation of azo dyes in the presence of TiO<sub>2</sub> doped with selective transition metals. *Desalination*. 2011;276:13–27.
  21. Mohammed Mastabur Rahman, Fatema Akthar Choudhury, Md. Delowar Hossain,

- Md. Namwarul Islam Chowdhury, Sadia Mohsin, Md. Mehdi Hasan, Md. Fakar Uddin, Niloy Chandra Sarker. Comparative study on the photocatalytic degradation of industrial dyes using modified commercial and synthesized TiO<sub>2</sub> photo catalysts. Journal of Chemical Engineering. 2012; 27(2):65-71.
22. Mphilisi M. Mahlambi, Ajay K. Mishra, Shivani B. Mishra, Rui W. Krause, Bhekie B. Mamba, Ashok M. Raichur. Metal doped nanosized titania used for the photocatalytic degradation of rhodamine B dye under visible-light. Journal of Nanoscience and Nanotechnology. 2013; 13:1–9.

---

© 2018 Lemessa et al.; This is an Open Access article distributed under the terms of the Creative Commons Attribution License (<http://creativecommons.org/licenses/by/4.0>), which permits unrestricted use, distribution, and reproduction in any medium, provided the original work is properly cited.

*Peer-review history:*  
*The peer review history for this paper can be accessed here:*  
<http://www.sciencedomain.org/review-history/28004>